Analytical Estimation and Experimental Validation of the Bending Stiffness of the Transmission Line Conductors

Hadiya Pritesh Dulabhai[*], *Parthasarathy N S*, *Gurumoorthy S Hebbar*
Department of Mechanical and Automobile Engineering,
CHRIST (Deemed to be University), Bengaluru-560074, Karnataka, INDIA
[*]*hadiyapriteshd@gmail.com*

ABSTRACT

The bending stiffness of transmission line conductors can vary significantly, ranging from maximum stiffness when behaving monolithically to minimum stiffness when wires behave loosely. This large range makes it challenging to estimate stiffness accurately at intermittent bending stages. To address this issue, a mathematical model that accounts for both frictional forces between wires in the same layer and the clenching effects of helical wires from preceding layers is proposed in this paper. The proposed model estimates cable bending stiffness as a function of axial load and curvature for multilayered strands by considering slip caused by wire behavior. To evaluate the bending stiffness, experiments were conducted on Panther and Moose Indian Power Transmission line conductors. The proposed slip model considers Coulomb frictional effects and clenching effects caused by Hertzian contact forces, filling the void in the estimation procedure. Additionally, the model considers the wire stretch effect, a parameter not previously accounted for in cable research. The predicted numerical results of the proposed model were found to vary within a maximum of 7% from the experimental tests. The proposed mathematical model thus offers a more accurate and comprehensive way of estimating the bending stiffness of transmission line conductors, addressing the existing limitations in the estimation procedure.

Keywords: *Bending Stiffness; Revised Slip Theory; Inter Wire Friction; Transverse Load*

ISSN 1823-5514, eISSN 2550-164X

https://doi.org/10.24191/jmeche.v21i1.25357

Received for review: 2023-03-01
Accepted for publication: 2023-08-16
Published: 2024-01-15

Introduction

The helically wound cables find extensive usage in overhead power transmission line applications all over the world. The conductors are formed with the central core assembly made of steel for withstanding the stringing tension and concentric layers of helical wires of aluminum, wound over the core assembly, and are used for electrical power transmission. Such conductors are known as Steel Reinforced Aluminum Conductors (ACSR) cables. Advancements in material technology have also resulted in All Alloy Aluminum Conductors (AAAC), composite conductors, and other new conductors with alternate materials. The structural assembly of such cables undergoes an axial pulling tension, and varying transverse bending curvatures, depending upon the mode of vibration of such cables due to the wind forces. The lateral response of such cables is influenced by the bending stiffness of the cable assembly which in turn depends upon the tribological interaction of the constituent wires, the frictional forces present in the contact locations, and the resistive mechanism offered at the wire interfaces. The accuracy of the response depends on the effectiveness of the mathematical model that considers the forces and moments that arise in the helical wire interfaces about its three mutually perpendicular axes. Though many mathematical models are stipulated in the last five or six decades in cables, seldom they consider the influence of wire forces and moments about its normal, bi-normal, and axial directions together, in any analysis and evaluation of the cable response. Though the dominant wire force and moments about the axial directions were never missed by many authors, due weightage of the contribution in the other two directions (normal and bi-normal) were not considered effectively, as a result of which the analytical predictions have not only become inaccurate but also lead to inconclusive results with some empirical relations. Though the global behavior of the cable apparently seems to be all right even with the omission of some forces/moments, the mechanism of its constituent wires needs a fully proven scientific explanation that predicts the local behavior also correctly. The ultimate response of the cable will be complete when accurate theories are attributed to global and local behaviors.

The effective stiffness of the cable assembly in its bent state varies widely between two extreme behaviors – a monolithic infinite friction state offering the maximum stiffness and a completely loose wire zero friction state offering the minimum thickness. Due to this wide variation, the estimation of the cable stiffness at any intermittent stage of bending has been under continuous refinement, a process that very much depends on the number of intricate parameters that are adopted by the researchers. Even though about 150 publications have been made over the last two decades on this trivial area, salient research that can be categorized and grouped is only presented in this paper to explain the gradual evolution and to emphasize the parameters that are included for refinement at various stages.

McConnell and Zemke [1] were the early investigators who conducted the experimental tests on overhead power transmission line conductors and observed a wide variation, of the order of 1:55 in their extreme values of the bending stiffness. This triggered interest in cable researchers to study the inner mechanism and propose analytical models that explain the bending behavior reasonably. Though fundamental mechanics relations for the equilibrium of the helical wires were established by Love [2], systematic analytical investigations began by the Costello [3] team in 1982. Treating the cable as an assembly of frictionless springs, Costello [4] improvised the Equations of Love and summarized his findings in his book. Sathikh [5] considered the internal friction forces that arise due to the twisting of the wires in a bent cable and formulated the expressions for the reduction of bending stiffness due to wire twists. The primary cause for this wire twist was observed to be the predominant axial force in the wire. Le-Clair and Costello [6] considered the axial friction force in the helical wires and predicted the stress and contact forces in a singled layered cable under the action of axial, torsional, and bending loads. When Papailiou [7] addressed the bending phenomenon of cables, the friction forces generated between the interlayers were also considered and a smooth transition of stiffness from stick to slip state was noticed. However, the axial force in the helical wire was considered to be the only cause in this analysis. Cardou [8] summarized the various models adopted for bending analysis in his review paper to that date. Sathikh et al. [9] for the first time, attempted to investigate the basic wire mechanics that resulted in the curvature and twist expressions and noticed the absence of a parameter called "wire stretch" influencing the successive bending and twisting of the helical wire. This parametrical inclusion of the wire stretch altered the basic curvature and twist relations of the helical wire and influenced the evaluation of wire moments in all its three axes. A single layered cable was analyzed for its pre-slip behavior and the maximum bending stiffness was re-estimated with these basic relations and found to be 16% lesser than the usual upper bound, monolithic stiffness estimation. This opened the need for considering certain intricate wire parameters that were ignored till this date. Hong [10] extended the Papailiou model to a multilayered cable but limited the analysis with wire axial force as the main contributor to the frictional effects. Spak [11] reviewed the various cable models summarized their findings and cited the role of friction and contact deformation in the helical wire of the strand, as a necessary parametric inclusion in cable research studies. This had created the much-needed spark in the cable researchers that followed later.

Foti and Martinelli [12] studied a cable subjected to tension torsion and bending loads and analyzed the friction forces arising in the wires from Coulomb stick friction theory but limited the study to those wires arranged in the layer only. Khan et al. [13] analyzed the bending behavior of multilayered spiral strands by considering the hoop contact force that arises between wires in the same layer and included the effect of contact deformation. Zheng et al.

[14] modeled the bending behavior of the spiral strands by considering the wire slippage caused by the bending loads. A gross slip criterion using the Coulomb hypothesis is formulated and the slippage of the wires is studied under the radial compression from the wires situated above. The basic Papailiou's analytical model considering the wire axial force as the main contributor for the slippage has been adopted by Zheng.

Recently, Zhou et al. [15] analyzed the effect of friction on the bending behavior of a single layered strand by considering the Coulomb friction hypothesis to model the slippage of the wires in the axial direction. The radial contact deformation of the helical wires and the central core wire had been considered to arrive at the deformed geometry. The axial slip at the helical wire interface had been studied and the reduction in the bending stiffness was evaluated as a function of cable axial loads. Though the analysis procedure had been simulated with a computer program, it did not consider the wire forces in the normal, and bi-normal directions and their moments, including the effects of radial clenching forces from the wires placed in the layers above. The bending curvatures had been introduced by imparting a transverse load arrangement on an axially loaded taut cable. The variation of the bending stiffness and the consequent deflection had been experimentally measured on a single layered cable for various axial load-transverse load combinations.

A quick review of the various bending models as of date indicates that the inter-wire slip among the helical wires has been addressed with the Coulomb friction force caused in the axial direction of the wire alone. Modes of slip in other wire directions were not considered. Though this may work fairly well on a single layered cable, it is not sufficient to analyze a multi-layered cable, where the slippage is not only caused by the Coulomb friction forces of the wires in the concerned layer alone but is also influenced by the radial clenching forces from the wires placed in the preceding layers. Even a few authors who studied the radial clenching effect due to the wires above, have not accounted for the effect of the same on the slip but have simply accounted for it with Coulomb friction theory only.

Noticing the above vital gap in cable bending research, Hadiya et al. [16]-[17] brought out two publications in which a revised cable bending model had been suggested to estimate the bending stiffness. The first publication, Hadiya et al. [16] included a parameter called 'wire stretch' that remains fundamentally in the straight wire before it takes successive stages of bending and twisting to form a helical path. When a cable is loaded, the change in normal and bi-normal curvature and the change in twist of the helical wire are influenced by the 'wire stretch' and hence alter the basic wire kinematic relations that are adopted to this date by all the researchers. Further, the shear displacement relation of the helical wire due to this 'wire stretch' has also been accounted for the first time in cable bending. All these revised fundamental kinematic relations have been formulated for a single layered cable and its maximum stiffness in the monolithic stage has been evaluated and compared

with the published results. A reduction of cable bending stiffness up to 5% has been noticed.

When a multi-layered cable under a higher axial load is bent, the radial clenching forces introduced from the wires in one layer to that in the adjacent layer beneath it, are significant enough to cause local deformation at the contact interfaces. This deformation can be addressed by the Hertzian contact theory. The slip caused by this additional deformation has also to be considered along with the usual slip that is estimated in the axial direction of the wire by Coulomb friction theory. While many authors have accounted for the axial slip due to Coulomb friction theory, Hadiya et al. [17] considered for the first time in cable bending the slip caused by the radial contact forces and accounted for the slippage of the helical wire due to the Coulomb friction forces and the Hertzian contact forces. The slip due to Coulomb friction theory has been addressed as a macro slip and the one due to Hertzian contact theory has been addressed as a micro slip. A novel slip model that combines the macro and the micro slip phenomenon has been suggested and the cable bending stiffness has been evaluated for a single layered cable as a function of bending curvature and compared with the recent works of Khan [13]. A maximum reduction of 4.34 % in bending stiffness has been noticed with the present model for a cable axial load of 10 kN

This paper is an extension of the analytical modeling of Hadiya [16]-[17] to a multilayered cable arrangement. The revised kinematic relations that include the 'wire stretch' effect have been extended to all the helical wires, placed in different layers of the strand, and the basic wire forces and moments have been accounted for with these improvised relations. The slippage of the wires in each layer has been considered to occur under the combined effects of macro and micro slip phenomenon. Special care has been taken to include the influence of radial clenching forces, introduced from the wires placed in the preceding layers. The bending moment in each layer has been evaluated by accounting for the respective status of no-slip, partial slip, or full slip, that exists at any bending curvature. The effective strand bending stiffness has been investigated as a function of curvature for two commonly used multilayered conductors - ACSR Panther and Moose for various axial loads of the cable. In order to validate the mathematical model, experimental tests are carried out on specially constructed test rigs that can accommodate a maximum span arrangement of 40 m. A transverse loading mechanism that can impart a vertical lateral load on the taut conductor has been fabricated. The lateral deflection of the conductor is measured at different locations of the conductor for various cable axial load-transverse load combinations. The detailed arrangement of the salient mathematical formulations is presented in the following section. The experimental test arrangement and the measurement procedure are elaborated. The bending stiffness evaluated from the measured deflections at these locations is compared with the analytical results of the revised combined slip theory. It is hoped that the new revised slip model will

be able to fill the void and predict the cable bending stiffness in a realistic manner.

Salient Mathematical Formulations

Revised kinematic relations

When a cable is applied with a tensile load, all the helical wires experience tensile force along their axes. When the wire is subsequently bent and twisted to take a helical path, the influence of the basic axial force and its consequent stretch is also carried out in the successive bending and twisting phenomenon. This is known as the 'wire stretch effect'. The revised kinematic relation of the wire curvatures in the normal and binormal directions ($\omega_{n\prime}, \omega_{b\prime}$) and the twist ($\omega_{t\prime}$) are presented in Equation (1) to Equation (3) for a helical wire at a position angle (ϕ).

$$\omega_{n\prime} = \kappa(\cos\beta\,(1+\sin^2\beta) - a_1\sin\beta\cos\beta + a_3\,sin^2\,\beta + a_2\sin\beta)\sin\phi \tag{1}$$

$$\omega_{b\prime} = \kappa(\cos^4\beta + a_1\sin\beta - a_2\,sin\,\beta\,cos\,\beta)\cos\phi \tag{2}$$

$$\omega_{t\prime} = \kappa(-\sin\beta\cos^3\beta + a_3\sin\beta + a_2\,sin^2\,\beta)\cos\phi \tag{3}$$

where κ is the total curvature of the strand, β is the lay angle, and a_1 , a_2 and a_3 factors defining shear strains and twists.

Revised slip model

The displacement or the slip of a helical wire at any contact interface is composed of a macro slip ($\bar{\Delta}_1$) initiated by the Coulomb friction effects and the micro slip ($\bar{\Delta}_2$) caused by the contact deformation of the radial clenching forces (X_0). This paper judiciously combines them as an equivalent spring in series arrangement, since both these slips are affected by the same source of wire axial force (T). The total bending curvature of the strand at any contact interface is obtained as:

$$\kappa = \kappa_1 + \kappa_2 = \kappa_1\left(1 + \left(\frac{\bar{\Delta}_2}{\bar{\Delta}_1}\right)\right) \tag{4}$$

where, κ_1 is the bending curvature pertaining to the axial force (T) sustained in the wire. The average value of the macro slip in the strand cross section is given by:

$$\bar{\Delta}_1 = \left(\frac{2}{\pi}\right) B\bar{Z}\kappa_1 \tag{5}$$

where,

$$B = \left[\frac{(r/R)^2}{E\pi \sin^2 \beta}\right] \tag{6}$$

$$\bar{Z} = EA \cos^2 \beta \sin \beta \tag{7}$$

where, *R*, *A*, and *E* are the radius, cross-section area, and elastic modulus of the wire, and *r* is the helix radius of the wire. The average value of the micro slip caused by the radial contact force (X_0) at any cross-section of the strand is given by:

$$\bar{\Delta}_2 = d\left(\frac{2}{\pi}\right)\int_0^{\pi/2}\left[1 - \left(1 - \frac{\bar{Z}\kappa_1 \, sin\, \phi}{\mu X_0}\right)^{2/3}\right] d\phi \tag{8}$$

where,

$$\mathrm{d} = \frac{3}{2}\left(\frac{\mu \mathrm{X}_0 S_{22}}{1 - \upsilon}\right) \tag{9}$$

is obtained from the tangential compliance S_{22} of the helical wire of Poisson ratio υ and μ is the co-efficient friction at the wired interface.

Slip regimes and curvatures

The helical wire at any cross section will undergo three stages of slips, namely- no slip, partial slip, or full slip depending on the applied axial force in the wire ($\bar{X}$) and the resisting friction force ($\mu \mathrm{X}_0$), caused by the normal contact force (X_0) at any surface with a friction coefficient (μ).

The wire will be in the monolithic state when the applied axial force is less than the resisting friction force, and as a limiting case, where these two forces become equal, slip is initiated at a wire position $\phi = 90^o$ located along the neutral axis. The slip initiation curvature is given by:

$$\kappa_o = \frac{\mu \mathrm{X}_0}{\bar{X}} \tag{10}$$

The progress of the slip will be initiated from this location and the wire will undergo a partial slip state when the position angle (ϕ_b) lies between 0^o to 90^o and the curvature of the partial slip state is identified as:

$$\kappa_b = \kappa_o \left(\frac{\frac{\pi}{2} - \phi_b}{\cos \phi_b} \right) \tag{11}$$

On further loading, the wire attains a full slip state at the curvature:

$$\kappa_f = \frac{\pi}{2} \kappa_o \tag{12}$$

Strand bending stiffness

The bending moment developed in any layer of the strand at any cross-section is a function of its bending curvature and the resultant summation of the moments of the individual wires, depending on their position angles, applied axial force (T), the resisting force, and their slip status.

The wires in the monolithic state as shown in Equation (10) will be acted upon with a bending moment given by:

$$M_T = \frac{m}{2} EAr^2 \kappa_1 \cos^3 \beta \tag{13}$$

where, the curvature κ_1 is below the limiting curvature κ_o and m is the number of wires in that layer. The wires, whose positions are lying between 0 to $\frac{\pi}{2}$, will be in the partial slip stage or full slip stage as dictated by Equations (11) and (12) depending on the resisting forces developed. Accordingly, the bending moment of such wires is given by:

$$M_{T_p} = \frac{m}{\pi} EA\kappa r^2 \cos^3 \beta \left[\emptyset_b + \frac{\sin 2\emptyset_b}{2} \right] \tag{14}$$

$$M_{T_s} = mr^2 \cot \beta \, \mu X_o \left(\frac{2}{\pi} \right) \left[\cos \emptyset_b + \emptyset_b \sin \emptyset_b - \frac{\pi}{2} \sin \emptyset_b \right] \tag{15}$$

The fully slipped wires at any cross-section are identified by Equation (12) and their corresponding bending moment is given by:

$$M_{T_f} = m \left(\frac{2}{\pi} \right) \mu \mathrm{X}_o r^2 \cot \beta \tag{16}$$

The layer bending moment of the strand at any cross-section due to the axial force (M_T) is the sum of the moments of the individual wires that are in no slip / partial slip or full slip stages as shown by Equations (14), (15), and

(16). The moment generated in a layer of strands due to the rolling of wires that are acted upon by the wire moments G, G' *and* H is given by:

$$M_G = m\left(\frac{2}{\pi}\right)\int_0^{\pi/2} EI\omega_{n'} \sin\phi \, d\phi \tag{17}$$

$$M_{G'} = m\left(\frac{2}{\pi}\right)\int_0^{\pi/2} EI\omega_{b'} \cos\beta \cos\phi \, d\phi \tag{18}$$

$$M_H = -m\left(\frac{2}{\pi}\right)\int_0^{\pi/2} GJ\omega_{t'} \sin\beta \cos\phi \, d\phi \tag{19}$$

where I and J are the area moment of inertia and polar moment of inertia of the helical wire. The layer bending moment at any cross-section of the strand due to the rotation of the wires can be obtained as:

$$M_r = M_G + M_{G'} + M_H \tag{20}$$

The net layer bending moment of the strand at any cross section can be obtained as a summation of the moments caused due to the axial force (M_T) and that due to the rotation of the wires (M_r).

$$M_{b_i} = M_T + M_r \tag{21}$$

The total bending moment in the strand at any cross-section, can then be obtained as the summation of the bending moments of all the layers and that of the central core as given by:

$$\mathrm{M_b} = \sum_{i=1}^{l} M_{b_i} + E_C I_C \kappa \tag{22}$$

where $'l'$ is the number of layers in the strand, $E_C I_C$ are the modulus of rigidity and the area moment of inertia of the core and κ is the total curvature of the strand. The strand bending stiffness at any cross-section of the strand can be obtained from the plot of M_b vs κ or from the relation:

$$EI_{strand} = M_b / \kappa \tag{23}$$

Numerical results of bending stiffness

The mathematical formulation discussed in the previous section is numerically worked out for two multilayered conductors – ACSR Panther (three layers and one central straight wire) and ACSR Moose (four layers and one central straight wire), whose specifications are mentioned in Table 1.

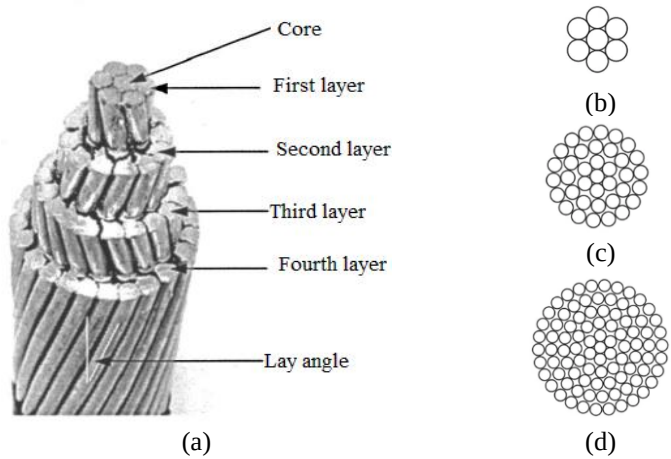

Figure 1: (a) Pictorial view of a multilayered cable and schematic cross-section diagrams of (b) a single layered cable, (c) a three layered cable, and (d) a five layered cable

The axial loads that are applied on these conductors are restricted to $25 \pm 5\%$ of their ultimate breaking strength, as those are the usual working loads, as per Indian Standard-398 [18] recommendations. The cable axial strain (ϵ), corresponding to this axial load is evaluated by treating the conductor to be in a monolithic state in accordance with its initial state. The bending curvature (κ_1) corresponding to a helical wire, placed at the outer layer is evaluated as per its axial and angular position in the strand.

Table 1(a): Material and geometrical properties of ACSR Panther conductor

Layer no.	Material	No. of wires	Wire diameter (mm)	Lay angle (degrees)	Young's modulus (N/mm^2)	Ultimate breaking load (kN)
1	Steel	1	3	0	207000	89.67
2		6	3	5.83	207000	
3	Aluminum	12	3	10.94	69000	
4		18	3	14.04	69000	

The axial strain ($\in_w$) in the helical wire located on the outermost layer at a particular cross-section is evaluated from its geometrical location and the wire axial force (T) and its corresponding radial clenching contact force (X_o) are evaluated. Depending on the friction coefficient between the materials of the outermost and the immediate wires placed below, the frictional resisting force is also evaluated. The limiting curvature at which slip is initiated in this wire as per the Coulomb friction theory is found in Equation (10). The status of slip in the other wires in this layer is investigated as per Equations (10) to (12) and the bending moment due to the axial force that causes axial slip is evaluated for all the wires in the outermost layer from the appropriate Equations (13) to (16). Due care was taken to include the effective slip caused by Coulomb friction theory (macro slip) and the one caused by micro slip due to the contact deformation of the wires as listed in Equations (1) to (9).

Table 1(b): Material and geometrical properties of ACSR Moose conductor

Layer no.	Material	No. of wires	Wire diameter (mm)	Lay angle (degrees)	Young's modulus (N/mm^2)	Ultimate breaking load (kN)
1	Steel	1	3.53	0.00	207000	
2	Steel	6	3.53	6.32	207000	
3		12	4.13	10.70	69000	159.6
4	Aluminum	18	4.13	11.70	69000	
5		24	4.13	13.10	69000	

The bending moment in the layer corresponding to the rotational movements of the helical wires is evaluated from Equations (17) to (19) and the net bending moment in the outer layer is calculated from Equations (20) and (21). The assembly of all the wires underneath this outermost layer is treated as a monolithic assembly and its stiffness is evaluated as mentioned in the works of Hadiya et al. [16]. The total stiffness of the strand is evaluated from Equations (22) and (23) after accounting for the center wire.

The status of slip at other cross sections of the cable is identified as per the procedure mentioned above, for all the wires in the outer layer as per the first portion of the cable stiffness vs curvature plot of Figure 2(a) pertaining to ACSR Panther conductor for an axial load specified for an axial load of 20% ultimate tensile stress.

By increasing the curvature further, the slip initiation curvature of the penultimate layer (the immediate inner layer of the outermost) is identified and the various slip stages are accounted for as the slip progresses and the layer bending stiffness is evaluated as that of the outer layer. The cable stiffness at this stage is the sum of the current penultimate layer stiffness the monolithic stiffness of the cable underneath this layer and the loose wire stiffness for the outer layer, which has fully slipped by now. The similar procedure is repeated

for all the other layers and finally, the central core wire stiffness is added to account for the total cable bending stiffness.

The complete stiffness distribution plot as a function of cable curvature is shown in Figure 2(a) for different axial loads namely 20%, 25%, and 30% UTS of the conductor as recommended in Indian Standard-398. A similar distribution plot is obtained for ACSR Moose as shown in Figure 2(b) The variation of the bending stiffness as a function of strand curvature confirmed the complete transition of the cable from a monolithic stick state to a loose wire gross slip state explaining the slip hypothesis adopted in this work.

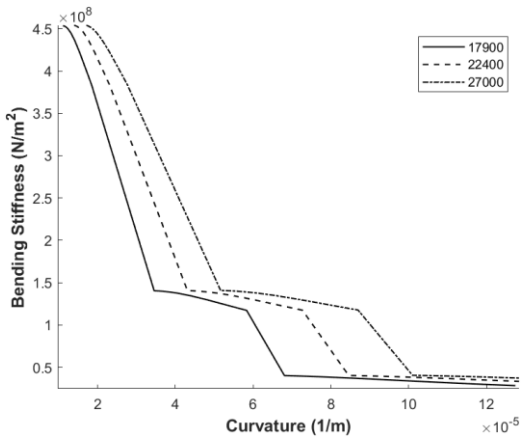

(a)

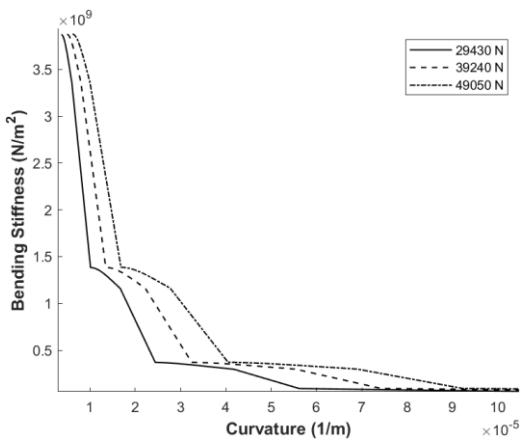

(b)

Figure 2: Strand bending stiffness-curvature plots for; (a) ACSR panther conductor, and (b) ACSR moose conductor

Experimental Evaluation of Bending Stiffness

Experimental setup and procedure

The analytical approach presented earlier in this discussion examines the bending stiffness of a conductor. To validate this, a bending curvature is introduced to the taut cable within a transmission line testing laboratory, facilitated by a transverse loading arrangement. Figure 3 illustrates the schematic diagram of the complete experimental setup.

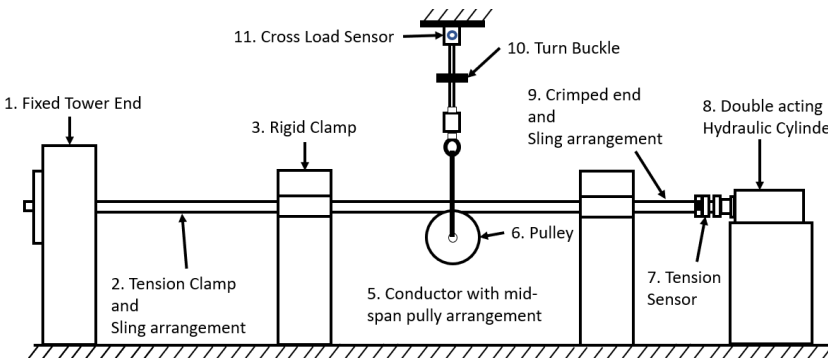

Figure 3: Schematic diagram of the experimental setup

Figure 4: (a) Conductor fixed end sling arrangement, (b) loading end hydraulic cylinder connected with a load sensor, (c) double ended hydraulic cylinder with load-cell and sling, and (d) transverse load sensor and turn buckle arrangement

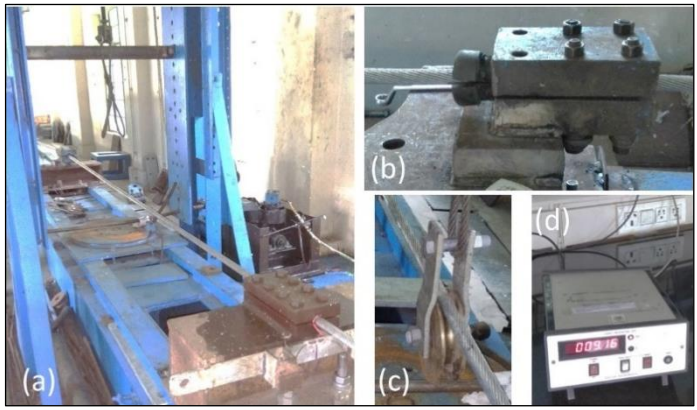

Figure 5: (a) conductor clamped at both ends with transverse load arrangement, (b) rigid clamp, (c) pulley arrangement to apply the transverse load at mid-span, and (d) load indicator

Initially, the conductor is loaded onto the experimental setup, with a fixed length of 3 meters and one end secured as shown in Figure 4(a), and the other end fixed with a hydraulic cylinder (Figure 4(b)) using a sling arrangement. After fixing, a horizontal pull is applied to keep the conductor in a taut condition with the help of a double-acting cylinder (Figure 4(c)). Once the conductor reaches the taut condition, an axial load is applied to it, which is limited to 25±5% of the conductor's breaking strength, as per the Indian Standard-398 specification. When the axial load is applied and stabilized, the conductor ends are clamped between two fixed supports (Figure 5(b)). Using a turnbuckle and cross-load sensor (Figure 4(d)), a transverse load is applied to the conductor mid-span through a pulley (Figure 5(c)). The applied axial load and cross load are measured by respective load cells and indicators installed in the setup. The deflections generated due to the transverse load within the conductor are measured at specified locations of 300, 600, 900, 1200, and 1500 mm. With the same axial load applied to the conductor, the transverse loads are increased in stages, and the corresponding deflections at various axial locations are measured using dial gauges. This procedure is repeated for different axial load-cross load combinations. These experiments are conducted with ACSR Panther and Moose conductors, and the resulting deflections are tabulated in Tables 2(a) and 2(b).

Analytical simulation of experimental arrangement

Figure 6 shows the schematic representation of the cable under the axial load (P), and a transvers load (Q).

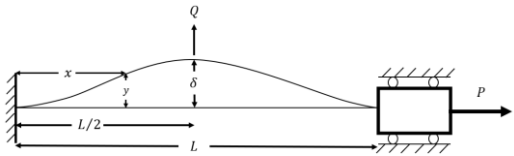

Figure 6: Schematic arrangement of the cable loading

The transverse deflection $y(x)$ at an axial position is given by:

$$y(x) = \frac{QL^3}{16EI\lambda^3}\left[\left(\frac{1-\cosh\lambda}{\sinh\lambda}\right)(1-\cosh bx) + (bx - \sinh bx)\right] \tag{24}$$

$$b = \sqrt{\frac{P}{EI}} \qquad \lambda = \frac{bL}{2} \tag{25}$$

where EI is the bending stiffness of the cable. The bending curvature corresponding to this location is given by:

$$y''(x) = \frac{QL^3}{16EI\lambda^3}\left[\left(\frac{1-\cosh\lambda}{\sinh\lambda}\right)(\cosh bx) + (\sinh bx)\right](-b^2) \tag{26}$$

Evaluation of deflections at different axial locations

It can be noted that the defection or the curvature at any location of the cable along the axis can be determined from Equations (24) and (26) if the appropriate value of the bending stiffness (EI) prevailing at that location is known. Bending stiffness values exhibit variations at different locations, influenced by curvatures and the degree of slippage on the bent cable. The detailed slip theories, as discussed earlier, explain this phenomenon. Figure 2 illustrates the variation of stiffness for Panther and Moose, portraying the relationship with cable curvatures.

If the stiffness of a cable at a particular location is to be calculated, the curvature of that location is to be known as apriori. In order to obtain the curvature and the corresponding stiffness and deflections of the cable at different axial positions along the cable, the following procedure is adopted.

1. The bending stiffness vs curvature plot is obtained as per the revised slip theory for a particular conductor for a known axial load (P) as shown in Figure 2.
2. The length of the conductor is divided into a suitable number of steps.
3. The curvature (y'') at the first step is calculated using Equation (26) by substituting the monolithic stiffness value for EI based on the Equation

reported by Hadiya et al. [16] for the known axial load (P) and the cross load (Q).

4. The stiffness value EI at this step is corrected from the stiffness curvature plot of the conductor (Figure 2(a) or 2(b)) by noting the curvature for this section on the horizontal axis and by obtaining the corresponding stiffness value from the plot on the vertical axis. It can be noted that a 5^{th} and 7^{th}-order data fit equation having the co-efficient of determination (R^2) of 0.96, is developed to capture the bending stiffness for any curvature accurately from the above plots.
5. The deflection of the first step is calculated from Equation (24) by using the revised value of EI obtained from Step 4.
6. The curvature at the next step is obtained from Equation (26) using the stiffness value of the previous section obtained in step 4 and the corresponding deflection at this section is calculated as in step 5.
7. The above procedure is repeated for all the points up to the desired location and the corresponding deflection is obtained.

Comparison of numerical and experimental results

Tables 2(a) and 2(b) show the measured transverse deflections of ACSR Panther and Moose conductors at different axial locations of 300, 600, 900, 1200, and 1500 mm for cross loads varying from 980 to 3000 N. The conductor span between the fixed support is maintained at 3 meters, with a constant axial load of 29420 N. The analytical results of deflections at these locations, evaluated as per the revised slip model presented in this paper and by following the procedure outlined in the previous sections, are tabulated alongside the experimental values in Table 2(a) and 2(b).

Table 2(a): Transverse deflection results for an axial load of 29420 N – ACSR Panther conductor

Transverse load in N	The position where displacements were is measured in mm									
	Experimental					Numerical				
	300	600	900	1200	1500	300	600	900	1200	1500
980	1.6	4.0	6.3	8.5	10.5	1.7	4.1	6.6	9.0	10.7
1470	3.6	8.5	13.0	18.2	22.0	3.8	8.8	13.8	18.8	22.5
1960	6.0	13.5	20.5	28.0	33.5	6.2	13.7	21.2	28.7	34.3
2450	9.0	19.0	29.0	39.5	45.0	8.7	18.7	28.7	38.7	44.5
2940	12.0	23.0	37.0	50.0	60.5	11.1	23.6	36.1	48.7	59.7

Figures 7 and 8 show the transverse load vs displacement plots for ACSR Panther and Moose conductors for two axial positions 300 mm and 900 mm. The numerically evaluated results as per the combined slip model adopted in this paper are plotted as a function of transverse load. The measured deflections are also plotted for the five-transverse loads of 980, 1470, 1960,

2450, and 2940 N used in the experimental tests. The predicted results are found to vary with a maximum of 7% from the experimental values. The displacement plots of the combined slip model are also compared with the predicted results of the loose wire approach and monolithic behavior models discussed in the recent works of Hadiya et al. [16].

Table 2(b): Transverse deflection results for an axial load of 29420 N – ACSR Moose conductor

Transverse load in N	The position where displacements were is measured in mm									
	Experimental					Numerical				
	300	600	900	1200	1500	300	600	900	1200	1500
980	2.2	4.8	8.5	16.0	22.0	2.3	5.0	8.9	17.2	23.2
1470	4.3	7.5	14.0	24.5	34.0	4.4	7.8	14.7	26.6	35.3
1960	6.5	11.5	21.0	35.0	45.0	6.8	12.0	21.3	36.0	46.0
2450	9.5	22.0	35.0	48.0	65.0	9.2	21.7	34.2	47.2	63.9
2940	11.5	25.0	40.0	55.0	70.0	11.0	24.1	39.0	52.7	68.0

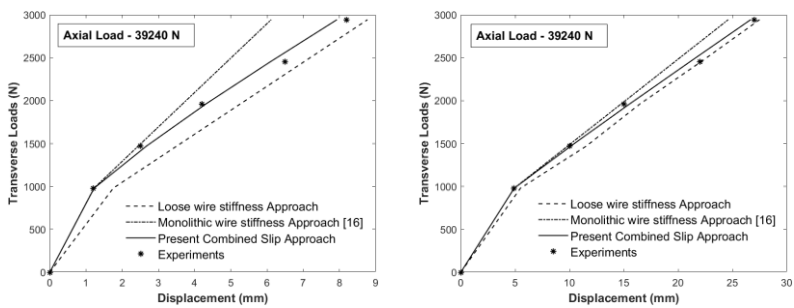

Figure 7: Transverse load vs. deflection for ACSR Panther conductor at; (a) 300 m, and (b) 900 m positions

It can be observed that when the transverse loads are minimal, the defection results agree with the monolithic approach. As the transverse loads are increased, the magnitude of slip increases, and the development of multiple slip regimes occurs, and the cable stiffness reduces and moves closer to the loose wire approach. Accordingly, the deflections are observed to be close to the loose wire behavior. In Figure 9 the displacements are plotted as a function of axial position for various transverse loads.

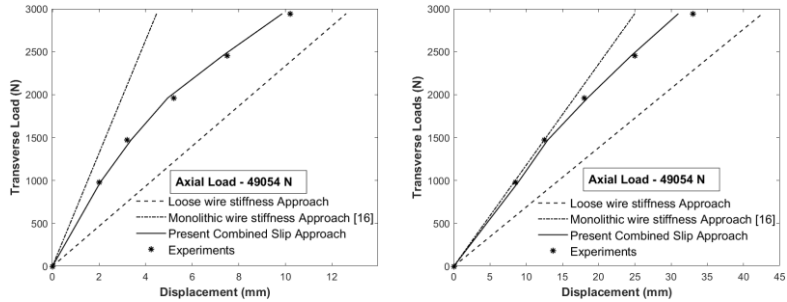

Figure 8: Transverse load vs. displacement for ACSR Moose conductor at; (a) 300 m, and (b) 900 m positions

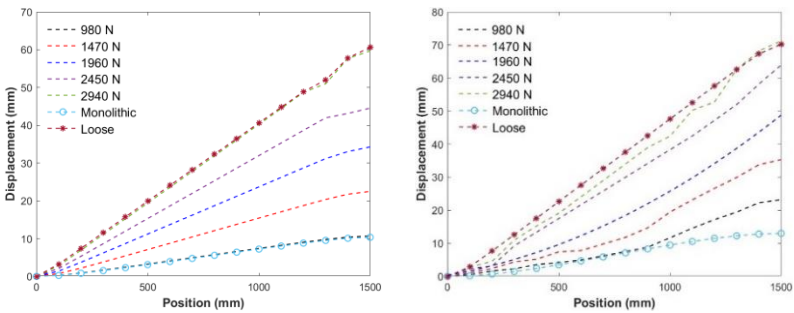

Figure 9: Displacement vs. axial position for various transverse loads; (a) Panter, and (b) Moose

Conclusions

Many models that are used to estimate the cable bending stiffness consider the slippage among the wires, due to the Coulomb frictional forces only. In the bending of multi-layer cables, the radial clenching forces, and their consequent deformation on the wires, are also responsible for estimating the extent of slippage. This paper considers this much-neglected aspect and estimates the slippage caused by the conventional coulomb frictional forces among the wire and that caused additionally by the clenching effects of the preceding layers placed above a helical wire, in any cable arrangement. The former is called macro slip and the later one is known as micro slip and the cable bending stiffness is evaluated with a judicial combination of the above as a spring in series arrangement. In addition, the basic cable kinematic relations that

describe the curvature and twist are revised with a parametric inclusion called the 'wire stretch effect', a fundamental physical happening in the wire under tension but consistently influencing the subsequent bending and twisting phenomena in the wires. Two ACSR multilayered cables-Panther and Moose used widely in Indian power transmission are considered for numerical evaluation and experimental verification of bending stiffness under various axial loads. The bending curvatures are introduced to the taut cables with a special transverse loading mechanism and the deflection of the cable along its selected axial locations is measured and compared with the numerical results. The major conclusions are outlined as under:

1. The slippage of the wire is initiated always on the outer layer first, among the wires placed near or on the neutral axis and progresses to other wires. With increased curvature the slip segments extend and the reduction in the bending stiffness occurs while the layer below maintains a monolithic state.
2. Subsequent increase in the cable curvature initiates slip in the wires located in the layer below and the wires undergo partial slip or full slip or their combinations and the cable stiffness reduce drastically as a function of curvature and attains a completely slipped loose wire state. The slip-initiating curvatures are found to increase with the cable axial loads and so the bending stiffness reduction.
3. The cable bending under the small transverse loads resembles a monolithic behavior and the stiffness is closer to the monolithic stiffness. This effect is pronounced more in cable under high axial loads.
4. When the transverse loads are increased and reach a threshold limit of an axial load combination, the cable behavior moves closer to the loose wire behavior, particularly on axial locations that are closer to the mid span.
5. The predicted results of transverse deflections of any axial position of a cable with the combined slip model of this paper are found to be closer to the experimentally measured value with a maximum variation of 7%.
6. The displacement versus the transverse load plots of the combined slip model suggested in this paper, indicate its adherence to a monolithic state when the cross loads are minimal, and the cable deflections move towards a loose wire state when the transverse loads are increased. At their threshold limits, they attain a complete loose wire behavior.

It is hoped that the refined kinematic parameters and the combined macro and micro slip theory adopted to estimate the stiffness of wires will enable a realistic estimation of cable bending stiffness by cable designers and researchers.

Contributions of Authors

The authors confirm the equal contribution in each part of this work. All authors reviewed and approved the final version of this work.

Funding

This work received no specific grant from any funding agency.

Conflict of Interests

All authors declare that they have no conflicts of interest

Acknowledgment

We express our gratitude to CHRIST (Deemed to be University), Bangalore, India, for inspiring and supporting our research efforts. Access to their data analysis software was crucial for conducting the analysis effectively.

References

[1] K. G. McConnell and W. P. Zemke, "The measurement of flexural stiffness of multistranded electrical conductors while under tension," *Experimental Mechanics*, vol. 20, no. 6, pp. 198–204, 1980. doi: 10.1007/BF02327599

[2] A. E. H. Love, "A treatise on the mathematical theory of elasticity," *Nature*, vol. 105, no. 2643, pp. 511–512, 1940. doi: 10.1038/105511a0

[3] G. A. Costello and G. J. Butson, "Simplified bending theory for wire rope," *Journal of the Engineering Mechanics Division*, vol. 108, no. 2, pp. 219–227, 1982. doi: 10.1061/(ASCE)0733-9399(1983)109:2(664)

[4] G. A. Costello, Theory of wire rope. Springer Science & Business Media, 1997.

[5] S. Sathikh and N. S. Parthasarathy, "Discussion of internal friction due to wire twist in bent cable," *Journal of Engineering Mechanics*, vol. 114, no. 4, p. 727, 1988. doi: 10.1061/(asce)0733-9399(1988)114:4(727)

[6] R. A. le Clair and G. A. Costello, "Axial, bending and torsional loading of a strand with friction," *Journal of Offshore Mechanics and Arctic Engineering*, vol. 110, no. 1, pp. 38–42, 1988. doi: 10.1115/1.3257121

[7] K. O. Papailiou, "On the bending stiffness of transmission line conductors," *IEEE Transactions on Power Delivery*, vol. 12, no. 4, pp. 1576–1588, 1997. doi: 10.1109/61.634178

[8] A. Cardou and C. Jolicoeur, "Mechanical models of helical strands," *Applied Mechanics Reviews*, vol. 50, no. 1, pp. 1–14, 1997. doi: 10.1115/1.3101684

[9] S. Sathikh, S. Rajasekaran, Jayakumar, and C. Jebaraj, "General thin rod model for preslip bending response of strand," *Journal of Engineering Mechanics*, vol. 126, no. 2, pp. 132–139, 2000. doi: 10.1061/(ASCE)0733-9399(2000)126:2(132)

[10] K.-J. Hong, A. Der Kiureghian, and J. L. Sackman, "Bending behavior of helically wrapped cables," *Journal of Engineering Mechanics*, vol. 131, no. 5, pp. 500–511, 2005. doi: 10.1061/(ASCE)0733-9399(2005)131:5(500)

[11] K. Spak, G. Agnes, and D. Inman, "Cable modeling and internal damping developments," *Applied Mechanics Reviews*, vol. 65, no. 1, p. 010801, 2013. doi: 10.1115/1.4023489

[12] F. Foti and L. Martinelli, "Mechanical modeling of metallic strands subjected to tension, torsion and bending," *International Journal of Solids and Structures*, vol. 91, pp. 1–17, 2016. doi: 10.1016/j.ijsolstr.2016.04.034

[13] S. W. Khan, B. Gencturk, K. Shahzada, and A. Ullah, "Bending behavior of axially preloaded multilayered spiral strands," *Journal of Engineering Mechanics*, vol. 144, no. 12, p. 4018112, 2018. doi: 10.1061/(asce)em.1943-7889.0001535

[14] X. Zheng, Y. Hu, B. Zhou, and J. Li, "Modelling of the hysteretic bending behavior for helical strands under multi-axial loads," *Applied Mathematical Modelling*, vol. 97, pp. 536–558, 2021. doi: 10.1016/j.apm.2021.04.004

[15] B. Zhou, Y. Hu, X. Zheng, and H. Zhu, "Bending Behavior of a Frictional Single-Layered Spiral Strand Subjected to Multi-Axial Loads: Numerical and Experimental Investigation," *Applied Sciences*, vol. 12, no. 9, p. 4792, 2022. doi: 10.3390/app12094792

[16] Dulabhai Hadiya Pritesh, N. S. Parthasarthy, and Gurumoorthy S Hebbar, "Evaluation of Maximum Bending Stiffness of Stranded Cables with Refined Kinematic Relations," *Advances in Manufacturing Engineering*, pp. 353–366, 2023.

[17] Dulabhai Hadiya Pritesh, N. S. Parthasarthy, and Gurumoorthy S Hebbar, "Improvised Model for Estimation of Cable Bending Stiffness Under Various Slip Regimes," *Advances in Manufacturing Engineering*, vol. 341, pp. 389–402, 2023.

[18] Bureau of Indian Standards, Indian Standard, Aluminium conductors for overhead transmission purposes – Specification, Part-2, Aluminium conductors, galvanized steel-reinforced, 1996.